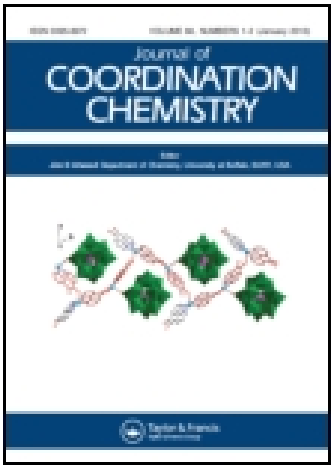

Journal of Coordination Chemistry
Publication details, including instructions for authors and subscription information:
http://www.tandfonline.com/loi/gcoo20

Assembly of two new polyoxometalate-templated supramolecular compounds by utilizing flexible 1,4-bis(pyrazol-1-ylmethyl)benzene ligand

Chunyan Zhao[ab], Huiyuan Ma[a], Haijun Pang[a], Shaobin Li[a], Yan Yu[ab], Tingting Yu[a] & Zhuanfang Zhang[ab]

[a] Key Laboratory of Green Chemical Engineering and Technology of College of Heilongjiang Province, College of Chemical and Environmental Engineering, Harbin University of Science and Technology, Harbin, PR China

[b] College of Chemistry and Chemical Engineering, Qiqihar University, Qiqihar, PR China

Accepted author version posted online: 18 Aug 2014.Published online: 02 Sep 2014.

To cite this article: Chunyan Zhao, Huiyuan Ma, Haijun Pang, Shaobin Li, Yan Yu, Tingting Yu & Zhuanfang Zhang (2014) Assembly of two new polyoxometalate-templated supramolecular compounds by utilizing flexible 1,4-bis(pyrazol-1-ylmethyl)benzene ligand, Journal of Coordination Chemistry, 67:17, 2820-2829, DOI: 10.1080/00958972.2014.953492

To link to this article: http://dx.doi.org/10.1080/00958972.2014.953492

Journal of Coordination Chemistry, 2014
Vol. 67, No. 17, 2820–2829, http://dx.doi.org/10.1080/00958972.2014.953492

Assembly of two new polyoxometalate-templated supramolecular compounds by utilizing flexible 1,4-bis (pyrazol-1-ylmethyl)benzene ligand

CHUNYAN ZHAO†‡, HUIYUAN MA*†, HAIJUN PANG*†, SHAOBIN LI†, YAN YU†‡, TINGTING YU† and ZHUANFANG ZHANG†‡

†Key Laboratory of Green Chemical Engineering and Technology of College of Heilongjiang Province, College of Chemical and Environmental Engineering, Harbin University of Science and Technology, Harbin, PR China
‡College of Chemistry and Chemical Engineering, Qiqihar University, Qiqihar, PR China

(*Received 8 April 2014; accepted 21 July 2014*)

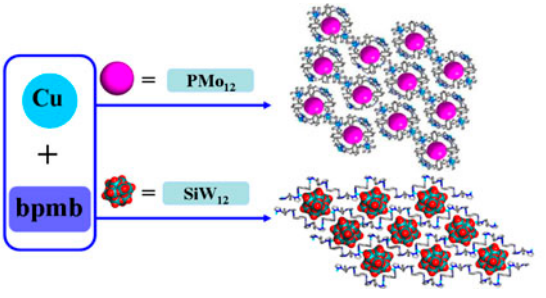

Two new POM-templated supramolecular compounds with good electrocatalytic activities toward reduction of iodate have been obtained, which shows that Keggin anions should play a significant role in the process of assembly.

Two new polyoxometalate-templated supramolecular compounds, $[Cu^{I}_4(bpmb)_4][PMo^{VI}_{11}Mo^{V}O_{40}]$ (**1**) and $[Cu^{I}_4(bpmb)_4SiW_{12}O_{40}]$ (**2**) (bpmb = 1,4-bis(pyrazol-1-ylmethyl)benzene), have been synthesized under hydrothermal conditions and characterized by routine methods. Structural analysis shows that in **1,** there exist crown-like $[Cu^{I}_4(bpmb)_4]$ coordination macrocycles, and the Keggin polyanions $[PMo^{VI}_{11}Mo^{V}O_{40}]^{4-}$ (abbr. as PMo_{12}), which direct the crown-like macrocycle to form a 3-D supramolecular framework. In **2,** there exist unusual meso-helix chains, and these chains are mutually interlaced in a wave–trough pattern, but without intersection resulting in a multi-cavity layer, in which the $[SiW_{12}O_{40}]^{4-}$ (abbr. as SiW_{12}) clusters as guest molecules occupy the cavities of the layers. The distinct structural features of the two compounds suggest that Keggin polyanions should play a significant role in the process of assembly. Electrocatalytic properties of **1** and **2** were investigated.

Keywords: Keggin; Polyoxometalate template; Crown-like macrocycle; Electrocatalytic properties

*Corresponding authors. Email: mahy017@163.com (H. MA); panghj116@163.com (H. Pang)

1. Introduction

Supramolecular hybrid compounds have drawn enormous attention because of their wide-ranging applications in solid electrolytes, catalysis, antitumor activities, separation materials, etc. [1–8]. An important synthetic strategy is the use of various anions as templates to build supramolecular hybrid compounds [9, 10]. Some small anions, such as ClO_4^-, PF_6^-, and X^- (X = Cl, Br, I) [11–15], have been used as templates; utilization of various large inorganic anions as templates to construct supramolecular hybrid compounds has become a prominent branch of this field. Polyoxometalates (POMs), exemplified by the ubiquitous spherical Keggin clusters, have been regarded as excellent candidates of templates to obtain hybrid compounds due to their structural diversity and superior potential applications, such as catalytic activity and electrochemistry [16–20]. In particular, recent results have indicated that these large POM anions as templates can be incorporated into the void space of conventional coordination frameworks, thereby offering a new opportunity for carrying out chemical reactions within the intercrystalline voids [21–28]. Exploration and construction of new POM-templated supramolecular compounds are a promising challenge for chemists.

Recently, flexible N-containing ligands have attracted interest in building POM-based hybrid compounds owing to their flexibility and conformational freedom [29–34]. Among the flexible ligands, we are currently interested in introducing 1,4-bis(pyrazol-1-ylmethyl) benzene (abbr. as bpmb) into our reaction system based on the following considerations: (i) bpmb possessing both flexible and rigid sites, in which the $-(CH_2)-$ part can provide a flexible role and the phenyl ring can afford a rigid site [35–39] and (ii) the flexible nature of $-(CH_2)_n-$ spacers allows the ligands to bend freely to satisfy the coordination requirement of metal centers. Thus, the bpmb molecules are good as ligands linking metal ions such as copper cations to form novel POM-templated supramolecular compounds [40, 41].

On the basis of the aforementioned points, by choosing bpmb, copper ions, and Keggin polyanions via the hydrothermal synthesis method, we constructed two new POM-templated compounds, $[Cu^I_4(bpmb)_4][PMo^{VI}_{11}Mo^{V}O_{40}]$ (**1**) and $[Cu^I_4(bpmb)_4SiW_{12}O_{40}]$ (**2**). Furthermore, the electrochemical and electrocatalytic behaviors of the two compounds have been studied.

2. Experimental methods

2.1. *Materials and general procedures*

All reagents were purchased from commercial sources and used without purification. Elemental analyses (C, H, and N) were performed on a Perkin-Elmer 2400 CHN Elemental Analyzer and that of W, Mo and Cu were performed on a PLASMA-SPEC(I) ICP atomic emission spectrometer. IR spectra were recorded from 4000 to 400 cm^{-1} on an Alpha Centaurt FT-IR spectrophotometer using KBr pellets. X-ray powder diffraction patterns were recorded on a Siemens D5005 diffractometer with CuKα (λ = 1.5418 Å) radiation. A CHI660 electrochemical workstation was used for control of the electrochemical measurements and data collection. A conventional three-electrode system was used with a modified carbon paste electrode (CPE) as a working electrode, a twisted platinum wire as counter electrode, and commercial Ag/AgCl as a reference electrode. The **1**- and **2**-CPEs were fabricated according to the method reported [42].

2.2. *Synthesis*

2.2.1. Synthesis of $[Cu^{I}_{4}(bpmb)_4][PMo^{VI}_{11}Mo^{V}O_{40}]$ (1). A mixture of $H_3PMo_{12}O_{40}$ (0.06 mM, 200 mg), $CuCl_2$ (0.50 mM, 67 mg), and bpmb (0.10 mM, 21 mg) were dissolved in 12 mL of distilled water. The resulting suspension was stirred for 0.5 h, and the pH was adjusted to 3.0 with 1.0 M L^{-1} HCl. Then, the suspension was sealed in an 18- mL Teflon-lined reactor and heated at 160 °C for 4 days. After cooling slowly (10 °C h^{-1}) to room temperature, red block crystals were obtained. The crystals were stable in air at ambient temperature and insoluble in common organic solvents and water (37% yield based on Mo). Anal. Calcd for $C_{56}H_{56}Cu_4N_{16}O_{40}PMo_{12}$ (**1**) (3029.62): C, 22.20; H, 1.86; N, 7.40; Cu, 8.39; Mo, 38.00 (%). Found: C, 22.25; H, 1.97; N, 7.34; Cu, 8.30; Mo, 37.87 (%).

2.2.2. Synthesis of $[Cu^{I}_{4}(bpmb)_4SiW_{12}O_{40}]$ (2). The preparation of **2** was similar to that of **1** except that $H_4SiW_{12}O_{40}$ (0.06 mM, 173 mg) was used instead of $H_3PMo_{12}O_{40}$. Red block crystals were obtained. The crystals were highly stable in air at ambient temperature and insoluble in common organic solvents and water (40% yield based on W). Anal. Calcd for $C_{56}H_{56}Cu_4N_{16}O_{40}SiW_{12}$ (**2**) (4089.08): C, 16.48; H, 1.38; N, 5.49; Cu, 6.23; W, 54.05 (%). Found: C, 16.59; H, 1.30; N, 5.58; Cu, 6.12; W, 53.89 (%).

2.3. *X-ray crystallography*

Single-crystal X-ray diffraction data for **1** and **2** were recorded on a Bruker Apex CCD diffractometer with graphite-monochromated Mo-Kα radiation (λ = 0.71069 Å). Absorption corrections were applied using multi-scan technique. All the structures were solved by the direct method of SHELXS-97 [43] and refined by full-matrix least-squares using the SHELXL-97 program [44]. The hydrogens of the organic ligands for **2** were refined as rigid groups. The detailed crystallographic data and structure refinement parameters are summarized in table 1.

Table 1. Crystal data and structure refinements for **1** and **2**.

Compounds	**1**	**2**
Formula	$C_{56}H_{56}Cu_4N_{16}O_{40}PMo_{12}$	$C_{56}H_{56}Cu_4N_{16}O_{40}SiW_{12}$
M	3029.62	4089.08
Crystal system	Monoclinic	Monoclinic
Space group	*C2/c*	*C2/c*
a (Å)	17.515(5)	18.228(5)
b (Å)	19.495(5)	22.470(5)
c (Å)	25.045(5)	22.666(5)
V (Å^3)	8249(4)	9263(4)
β (°)	105.303(5)	93.785(5)
Z	4	4
T (K)	296(2)	296(2)
μ (mm^{-1})	2.811	15.833
F(0 0 0)	5836.0	7496.0
GoF on F^2	1.119	0.930
R_1[a]/wR_2[b] [$I \geq 2\sigma(I)$]	0.0934/0.2476	0.0774/0.1646

[a]$R_1 = \sum||F_o| - |F_c||/\sum|F_o|$.
[b]$wR_2 = \sum[w(F_o^2 - F_c^2)^2]/\sum[w(F_o^2)^2]^{1/2}$.

3. Results and discussion

3.1. *Structure description*

3.1.1. $[Cu^{I}_4(bpmb)_4][PMo^{VI}_{11}Mo^{V}O_{40}]$ (1). Single-crystal X-ray diffraction analysis reveals that **1** crystallizes in the monoclinic space group *C2/c* (No. 15) and the structure of **1** is a 3-D supramolecular framework. The asymmetric unit of **1** consists of one non-coordinated PMo_{12} global cluster and one $[Cu_4(bpmb)_4]^{4+}$ crown-like macrocycle (figure 1). The PMo_{12} cluster exhibits a classical α-Keggin configuration [45], consisting of central PO_4 tetrahedron with corner-sharing four-triad $\{Mo_3O_{13}\}$ clusters. The central four μ_4-O atoms are observed to be disordered over eight positions with each oxygen site half-occupied, which is usual for Keggin clusters [46–48]. The P–O bond lengths are 1.43(2)–1.65 (3) Å, and the Mo–O bond lengths are 1.65(2)–2.49(2) Å. All of the bond lengths are within the normal ranges and in close agreement with those described in the literature [49, 50].

In the $[Cu^{I}_4(bpmb)_4]^{4+}$ subunit, there are three crystallographically independent Cu cations (two $Cu1^{+}$, one $Cu2^{+}$, and one $Cu3^{+}$) and four bpmb ligands. All Cu^{+} ions show identical linear coordination geometry coordinated by two nitrogens from different bpmb ligands with Cu–N distances ranging from 1.83(3) to 1.84(2) Å, within the normal ranges observed in other Cu(I) complexes [40, 41]. Generally, bpmb possesses two types of conformations: "Z"-type *trans*-conformation with two imidazole groups extending to opposite sides of the benzene ring and "U"-type *syn*-conformation with two imidazole groups extending to one side of the benzene ring [51, 52] (figure S1, see online supplemental

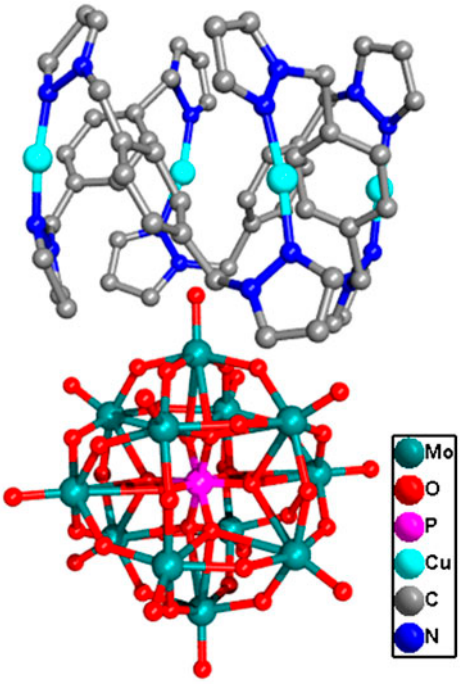

Figure 1. Ball/stick representation of the asymmetric unit of **1**. The hydrogens and crystal water molecules are omitted for clarity.

material at http://dx.doi.org/10.1080/00958972.2014.953492). In $[Cu^{I}_{4}(bpmb)_4]^{4+}$ subunit, the four crystallographically independent bpmb ligands adopt "Z"-type *trans*-conformation (figure S2a) and each bpmb links two Cu ions. As a result, a crown-like macrocycle is formed (figure S2b). There is a big cavity in the macrocycle, and the effective size is ca 9.497 Å × 9.825 Å (figure S2a). Because the diameter of the PMo_{12} cluster (ca. 10.4 Å) is longer than the aperture of cavity, the PMo_{12} cluster cannot be enwrapped absolutely by the cavity, which as guest molecule locates in the interspace between two adjacent $[Cu^{I}_{4}(bpmb)_4]^{4+}$ macrocycles. There exist hydrogen bonds between the neighboring PMo_{12} clusters and $[Cu^{I}_{4}(bpmb)_4]^{4+}$ macrocycles, such as O15···H18A–C18 (2.573 Å) and O20···H3A–C3 (2.635 Å), and as a result, the PMo_{12} clusters and $[Cu^{I}_{4}(bpmb)_4]^{4+}$ macrocycles are linked in a ABAB fashion to form a 1-D chain [figure 2(a)]. These chains are further connected through hydrogen bonds of O14···H1A–C1 (2.645 Å) to obtain a 3-D supramolecular framework [figure 2(b) and (c)].

3.1.2. $[Cu^{I}_{4}(bpmb)_4SiW_{12}O_{40}]$ (2). Single-crystal X-ray diffraction analysis reveals that **2** consists of one SiW_{12} cluster, four Cu^{I} ions, and four bpmb ligands as shown in figure 3. There are two crystallographically unique Cu ions with different coordination modes. $Cu^{I}(1)$ shows a linear coordination geometry by two nitrogens from different bpmb ligands. $Cu^{I}(2)$ displays a T-shaped configuration that is coordinated by two nitrogens from different bpmb ligands and one oxygen from a SiW_{12} anion. The Cu–N bond lengths are 1.88(3)–1.91(5) Å. All of these bond lengths are within the normal ranges observed in other Cu(I) complexes [40, 41]. After further investigation of the structures of **1** and **2**, we found that **2** is different from **1**, with bpmb ligands adopting two kinds of conformations in **2**: the

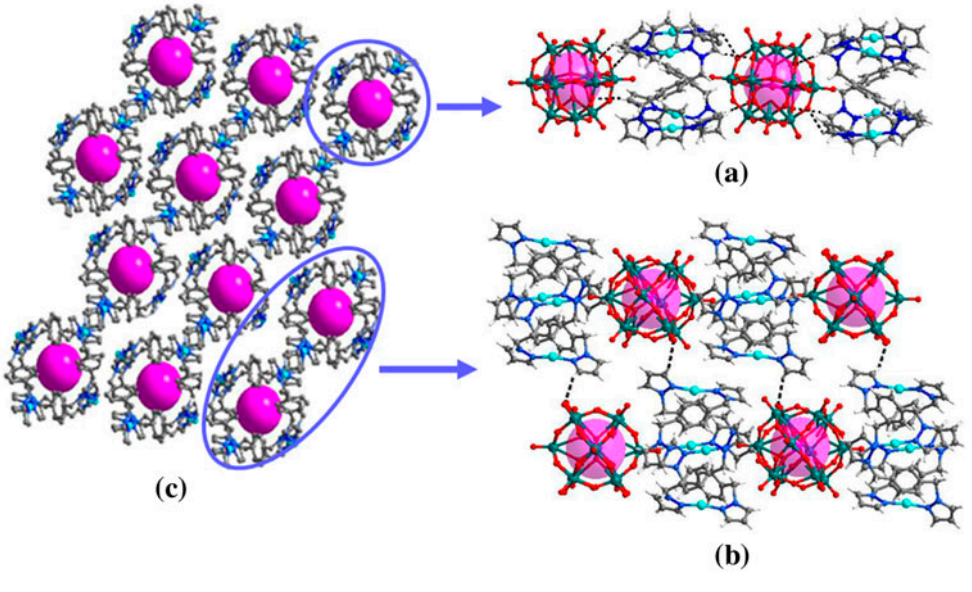

Figure 2. View the structure motifs in **1**: (a) a supramolecular chain consists of PMo_{12} clusters and $[Cu^{I}_{4}(bpmb)_4]^{4+}$ macrocycles, (b) view of hydrogen bonds between adjacent chains, and (c) a 3-D supramolecular framework.

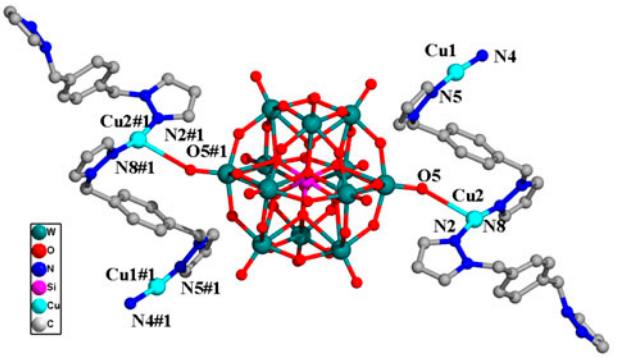

Figure 3. Ball/stick representation of the asymmetric unit of **2**. The hydrogens are omitted for clarity. Symmetry code: #1: $x, -1 + y, z$.

"U"-type *syn*-conformation and the "Z"-type *trans*-conformation; "U"- and "Z"-type bpmb ligands are alternately linked together via linkages of Cu(1) and Cu(2) ions to form a meso-helix chain (figure S3). Such a meso-helix chain was rarely reported, especially in POM system [53, 54]. Adjacent meso-helix chains are mutually interlaced in a wave–trough pattern, but without intersection to result in a multi-cavity layer, in which approximate elliptical windows are formed with effective size of ca 13.2 Å × 15.2 Å. The SiW_{12} clusters as guest molecules occupy the cavities of layers and are further incorporated via weak Cu–O interactions ($Cu^{I}(2)\cdots O(5)$ = 2.806(4) Å) (figure 4).

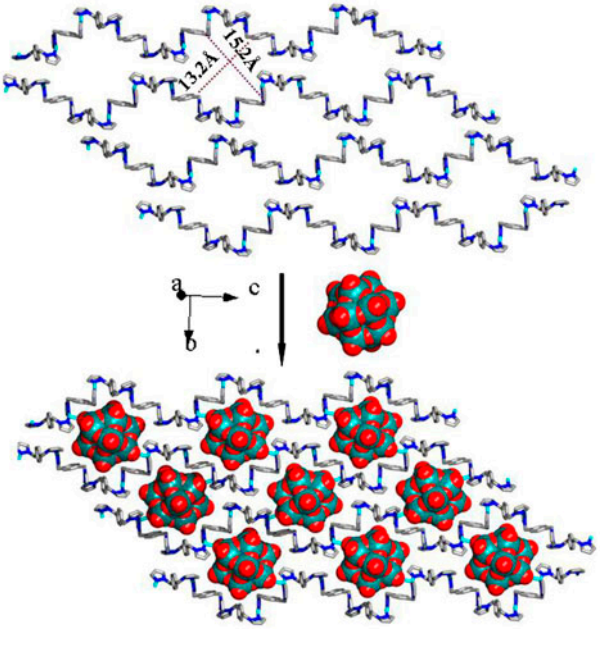

Figure 4. The 2-D POM-templated layer in **2**. The hydrogens are omitted for clarity.

3.1.3. Influence of the polyoxoanions on the structures of 1 and 2. Compounds **1** and **2** were synthesized under identical reaction conditions, except for the different clusters: PMo_{12} and SiW_{12}. These two clusters have the same structure, but different negative charge and a little different anion volume. Their negative charges are −3 and −4 and spherical diameters are ca. 10.48 Å and ca. 10.37 Å for PMo_{12} and SiW_{12}, respectively. Despite such small difference in these two starting POM clusters, these two new compounds have very different structures. In **1**, the PMo_{12} polyanions direct the [Cu(L)] coordination polymers to array around them with the L ligands adopting the "Z"-type *trans*-conformation, which results in crown-like channels [figure 2(a)]. In **2**, the ligands adopt both "Z"-type *trans*-conformation and "U"-type *syn*-conformation to conform with the SW_{12} polyanions, so a framework with 1-D meso-helix chain is obtained, in which the SW_{12} anions as templates are incorporated into the void space of the framework (figure 4).

3.2. *Analyses of bond valence sum, XPS, IR, and PXRD measurements*

3.2.1. Bond valence sum calculations and XPS. To confirm the valence of metals in **1** and **2**, the bond valence sum calculations (BVS) [55] have been made. The BVS calculations show that all Cu ions in **1** and **2** are in the +I oxidation states. The generation of Cu^{I} ions in **1** and **2** should be attributed to redox reaction of Cu^{II} ions and N-containing ligands (bpmb in this article), which occasionally occurs under hydrothermal conditions [34, 56]. From the results of the BVS calculations, we can see that all W ions are in the +VI oxidation states in **2**, whereas one Mo ion is in the +V oxidation state and the other eleven are in the +VI oxidation states in **1**. The mixed-valence state of Mo in **1** was further confirmed by XPS measurement. The XPS spectra of **1** are shown in figure S4. The XPS spectra exhibit peaks at 231.0, 232.0, 233.8, and 235.0 eV, attributed to Mo^{+V} $3d_{5/2}$, Mo^{+VI} $3d_{5/2}$, Mo^{+V} $3d_{3/2}$, and Mo^{+VI} $3d_{3/2}$, respectively [57, 58]. All the above results are consistent with the structural analyses and charge balance.

3.2.2. IR and PXRD. As shown in figure S5, IR spectra exhibit the characteristic peaks of α-Keggin structure at 1052, 953, 875, and 798 cm^{-1} in **1** as well as 1073, 953, 912, and 784 cm^{-1} in **2**, which are attributed to $\nu(X–O_c)$, $\nu(M=O_t)$, $\nu_{as}(M–O_b–M)$, and $\nu_{as}(M–O_c–M)$ (X = P, M = Mo, for **1**; X = Si, M = W, for **2**), respectively [34]. Bands in the 1259–1620 cm^{-1} region can be assigned to characteristic peaks of bpmb [40, 41].

The PXRD patterns for **1** and **2** are presented in figure S6. The diffraction peaks of both calculated and experimental patterns match well, indicating that the phase purities of **1** and **2** are good. The difference in reflection intensities between the simulated and the experimental patterns may be due to different orientation of the crystals in the powder samples.

3.3. *Electrochemical properties*

3.3.1. Voltammetric behavior of 1- and 2-CPEs. To study the redox properties of **1** and **2**, the CPEs (**1**-CPE and **2**-CPE) were prepared. The electrochemical behaviors were studied in 0.5 M H_2SO_4 solution at 50 mV s^{-1} scan rate. For **1**-CPE, as shown in figure 5(a), in the potential range −150 to +550 mV, there exist three quasi-reversible redox waves with half-wave potentials $E_{1/2} = (E_{pa} + E_{pc})/2$, 370 (I–I′), 206 (II–II′), and −14 (III–III′) mV,

respectively. The three redox waves correspond to three consecutive two-electron reductions of Mo^{VI} [59, 60]. However, the oxidation peak of copper centers is not observed from −150 to +550 mV. This phenomenon is also observed in similar Mo/Cu systems [34, 61, 62]. For **2**-CPE, as shown in figure 5(b), from +150 to −700 mV, there exist four pairs of quasi-reversible redox peaks with mean peak potentials, $E_{1/2} = (Ep_a + Ep_c)/2$, +431 (I–I′), +68 (II–II′), −483 (III–III′), and −639 (IV–IV′) mV, respectively. The first pairs of reversible redox peaks (I–I′) can be assigned to oxidation of Cu(I) [21] and other pairs of redox peaks should be ascribed to the three consecutive two-electron processes for SiW_{12} in **2** [63].

3.3.2. Electrocatalytic properties. The electrocatalytic properties of **1**- and **2**-CPEs have been investigated, and the results show that **1** and **2** have good electrocatalytic activities toward reduction of iodate (KIO_3) ascribed to Mo-centers or W-centers [64, 65]. As shown in figure 6(a) and (b), with addition of KIO_3, the reduction peak currents II′ of **1**- and **2**-CPEs increase gradually, while the corresponding oxidation peak currents decrease. The

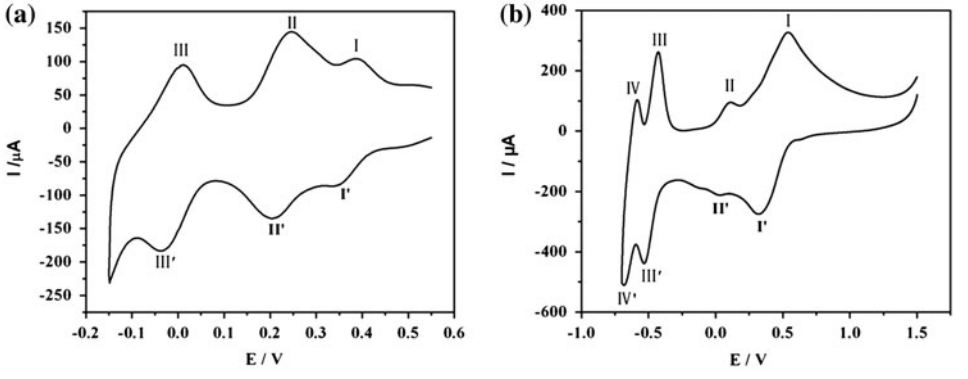

Figure 5. The cyclic voltammograms of **1**-CPE (a) and **2**-CPE (b) in 0.5 M H_2SO_4 solution.

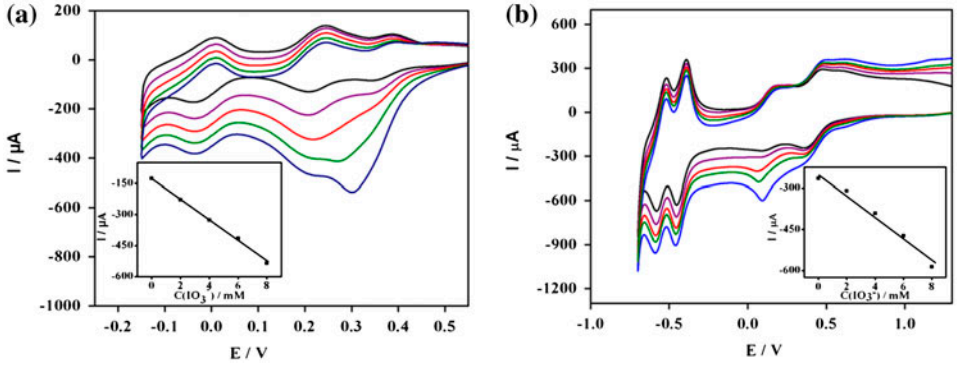

Figure 6. Reduction of $[IO_3]^-$ at **1**-CPE (a) and **2**-CPE (b) in 0.5 M H_2SO_4 solution containing $[IO_3]^-$ in various concentrations (from top to bottom): 0, 2, 4, 6, and 8 mM. The inset shows a linear dependence of the cathodic catalytic current of wave II with $[IO_3]^-$ concentration.

nearly equal current steps for each addition of KIO_3 demonstrate stable and efficient electrocatalytic activities of **1**- and **2**-CPEs. Furthermore, the electrocatalytic efficiency (CAT) of **1**-CPE and **2**-CPE can be roughly calculated by using CAT formula [66]. The results show that the CAT value toward the oxidation of KIO_3 is ca 550% and 130%, respectively, which suggest that **1** has potential applications in detection of KIO_3.

4. Conclusion

By tuning the POM clusters, two new POM-templated inorganic–organic supramolecular hybrid compounds are synthesized in the same Cu/bpmb system. The compounds provide intriguing examples of POM-templated hybrid compounds with good electrocatalytic activities toward reduction of iodate, show a feasible route to approach distinct structures by tuning the kinds of Keggin POM synthons, and open up possibilities for design of new POM-templated compounds with a simple synthetic strategy.

Supplementary material

Crystallographic data for the structure reported in this article have been deposited in the Cambridge Crystallographic Data Center with CCDC Numbers: CCDC-991328 (**1**) and CCDC-991329 (**2**) containing supplementary crystallographic data for this article. Other supplementary data associated with this article: IR data and additional structural figures of **1** and **2**, can be found in the online version.

Funding

This work was financially supported by the Foundation of Education Committee of Heilongjiang [grant number 12521072].

References

[1] H.J. Du, Z.Z. Shu, Y.Y. Niu, L.S. Song, Y. Zhu. *J. Solid State Chem.*, **190**, 296 (2012).
[2] J.Q. Sha, P. Yang, M. Chen, C.J. Li, L.J. Sun, D.W. Wang. *J. Coord. Chem.*, **66**, 3839 (2013).
[3] D.B. Dang, Y. Zheng, Y. Bai, X.Y. Guo, P.T. Ma, J.Y. Niu. *Cryst. Growth Des.*, **12**, 3856 (2012).
[4] Z.G. Han, Y.Z. Gao, X.L. Zhai, J. Peng, A.X. Tian, Y.L. Zhao, C.W. Hu. *Cryst. Growth Des.*, **9**, 1225 (2009).
[5] Y. Ding, J.X. Meng, W.L. Chen, E.B. Wang. *CrystEngComm.*, **13**, 2687 (2011).
[6] I. Efremenko, R. Neumann. *J. Am. Chem. Soc.*, **134**, 20669 (2012).
[7] A. Proust, B. Matt, R. Villanneau, G. Guillemot, P. Gouzerh, G. Izzet. *Chem. Soc. Rev.*, **41**, 7605 (2012).
[8] T. Hirano, K. Uehara, K. Kamata, N. Mizuno. *J. Am. Chem. Soc.*, **134**, 6425 (2012).
[9] C. Inman, J.M. Knaus, S.W. Keller. *Chem. Commun.*, 156 (2002).
[10] L.C. Tabares, J.A.R. Navarro, J.M. Salas. *J. Am. Chem. Soc.*, **123**, 383 (2001).
[11] M.R. Sambrook, P.D. Beer, J.A. Wisner, R.L. Paul, A.R. Cowley. *J. Am. Chem. Soc.*, **126**, 15364 (2004).
[12] S.S. Li, H.J. Yan, L.J. Wan, H.B. Yang, B.H. Northrop, P.J. Stang. *J. Am. Chem. Soc.*, **129**, 9628 (2007).
[13] R. Vilar, D.M.P. Mingos, A.J.P. White, D.J. Williams. *Angew. Chem. Int. Ed.*, **37**, 1258 (1998).
[14] A. Müller, H. Reuter, S. Dillinger. *Angew. Chem., Int. Ed. Engl.*, **34**, 2328 (1995).
[15] X.G. Yang, C.B. Knobler, M.F. Hawthorne. *J. Am. Chem. Soc.*, **114**, 380 (1992).
[16] Z.Y. Zhang, Q.P. Lin, D. Kurunthu, T. Wu, F. Zuo, S.T. Zheng, C.J. Bardeen, X.H. Bu, P.Y. Feng. *J. Am. Chem. Soc.*, **133**, 6934 (2011).
[17] X.L. Wang, Y.F. Wang, G.C. Liu, A.X. Tian, J.W. Zhang, H.Y. Lin. *Dalton Trans.*, 9299 (2011).

[18] S. Reinoso, M.G. Marqués, J.R. Mascarós, P. Vitoria, J.M. Zorrilla. *Angew. Chem. Int. Ed.*, **49**, 8384 (2010).
[19] J. Song, Z. Luo, D.K. Britt, H. Furukawa, O.M. Yaghi, K.I. Hardcastle, C.L. Hill. *J. Am. Chem. Soc.*, **133**, 16839 (2011).
[20] M.L. Qi, K. Yu, Z.H. Su, C.X. Wang, C.M. Wang, B.B. Zhou, C.C. Zhu. *J. Coord. Chem.*, **66**, 3531 (2013).
[21] P.P. Zang, J. Peng, J.Q. Sha, A.X. Tian, H.J. Pang, Y. Chem, M. Zhu. *CrystEngComm.*, **11**, 902 (2009).
[22] X.Y. Zhao, D.D. Liang, S.X. Liu, C.Y. Sun, R.G. Cao, C.Y. Gao, Y.Y. Ren, Z.M. Su. *Inorg. Chem.*, **47**, 7133 (2008).
[23] J. Guo, J. Yang, Y.Y. Liu, J.F. Ma. *Inorg. Chim. Acta*, **400**, 51 (2013).
[24] C. Inman, J.M. Knaust, S.W. Keller. *Chem. Commun.*, 156 (2002).
[25] D.D. Wang, J. Peng, H.J. Pang, P.P. Zhang, X. Wang, M. Zhu, Y. Chen, M.G. Liu, C.L. Meng. *Inorg. Chim. Acta.*, **379**, 90 (2011).
[26] Y.G. Li, L.M. Dai, Y.H. Wang, X.L. Wang, E.B. Wang, Z.M. Su, L. Xu. *Chem. Commum.*, 2593 (2007).
[27] B.X. Dong, J. Peng, C.L. Gómez-García, S. Benmansour, H.Q. Jia, N.H. Hu. *Inorg. Chem.*, **46**, 5933 (2007).
[28] X.L. Wang, C. Xu, H.Y. Lin, G.C. Liu, S. Yang, Q. Gao, A.X. Tian. *CrystEngComm.*, **14**, 5836 (2012).
[29] X.L. Wang, H.L. Hu, G.C. Liu, H.Y. Lin, A.X. Tian. *Chem. Commun.*, **46**, 6485 (2010).
[30] J.X. Meng, Y. Lu, Y.G. Li, H. Fu, E.B. Wang. *Cryst. Growth Des.*, **9**, 4116 (2009).
[31] Y.Q. Lan, S.L. Li, X.L. Wang, K.Z. Shao, D.Y. Du, H.Y. Zang, Z.M. Su. *Inorg. Chem.*, **47**, 8179 (2008).
[32] H. Fu, Y.G. Li, Y. Lu, W.L. Chen, Q. Wu, J.X. Meng, X.L. Wang, Z.M. Zhang, E.B. Wang. *Cryst. Growth Des.*, **11**, 458 (2011).
[33] P.P. Zhang, J. Peng, H.J. Pang, J.Q. Sha, M. Zhu, D.D. Wang, M.G. Liu, Z.M. Su. *Cryst. Growth Des.*, **11**, 2736 (2011).
[34] A.X. Tian, J. Ying, J. Peng, J.Q. Sha, H.J. Pang, P.P. Zhang, Y. Chen, M. Zhu, Z.M. Su. *Cryst. Growth Des.*, **10**, 1104 (2010).
[35] L. Zhang, X.Q. Lu, C.L. Chen, H.Y. Tan, H.X. Zhang, B.S. Kang. *Cryst. Growth Des.*, **5**, 283 (2005).
[36] L.L. Wen, Y.Z. Li, Z.D. Lu, J.G. Lin, C.Y. Duan, Q.J. Meng. *Cryst. Growth Des.*, **6**, 530 (2006).
[37] Z.D. Lu, L.L. Wen, Z.P. Ni, Y.Z. Li, H.Z. Zhu, Q.J. Meng. *Cryst. Growth Des.*, **7**, 268 (2007).
[38] Z.F. Tian, J.G. Lin, Y. Su, L.L. Wen, Y.M. Liu, H.Z. Zhu, Q.J. Meng. *Cryst. Growth Des.*, **7**, 1863 (2007).
[39] Y.Y. Liu, J.F. Ma, J. Yang, Z.M. Su. *Inorg. Chem.*, **46**, 3027 (2007).
[40] G.F. Hou, L.H. Bi, B. Li, L.X. Wu. *Inorg. Chem.*, **49**, 6474 (2010).
[41] G.F. Hou, L.H. Bi, B. Li, L.X. Wu. *Cryst. Growth Des.*, **13**, 3526 (2011).
[42] Z.G. Han, Y.L. Zhao, J. Peng, Y.H. Feng, J.N. Yin, Q. Liu. *Electroanalysis*, **17**, 1097 (2005).
[43] G.M. Sheldrick. *SHELXS-97, Program for the Solution of Crystal Structure*, University of Göttingen, Madison, MI (1997).
[44] G.M. Sheldrick. *SHELXTL 6.10*, Bruker Analytical Instrumentation, Madison, WI (2000).
[45] J.F. Keggin. *Nature*, **132**, 908 (1993).
[46] G.G. Gao, L. Xu, W.J. Wang, X.S. Qu, H. Liu, Y.Y. Yang. *Inorg. Chem.*, **47**, 2325 (2008).
[47] H.T. Evans, M.T. Pope. *Inorg. Chem.*, **23**, 501 (1984).
[48] H.J. Pang, J. Peng, C.J. Zhang, Y.G. Li, P.P. Zhang, H.Y. Ma, Z.M. Su. *Chem. Commun.*, **46**, 5097 (2010).
[49] Y.P. Ren, X.J. Kong, X.Y. Hu, M. Sun, L.S. Long, R.B. Huang, L.S. Zheng. *Inorg. Chem.*, **45**, 4016 (2006).
[50] J.Q. Sha, T.Y. Zheng, E.L. Zhang, H.B. Qiu, M.Y. Liu, H. Zhao, H. Yuan. *J. Coord. Chem.*, **66**, 977 (2013).
[51] Y. Qi, F. Luo, S.R. Batten, Y.X. Che, J.M. Zheng. *Cryst. Growth Des.*, **8**, 2806 (2008).
[52] C. Qin, X.L. Wang, E.B. Wang, Z.M. Su. *Inorg. Chem.*, **47**, 5555 (2008).
[53] C.J. Zhang, H.J. Pang, Q. Tang, H.Y. Wang, Y.G. Chen. *Inorg. Chem. Commun.*, **14**, 731 (2011).
[54] L. Han, M.C. Hong. *Inorg. Chem. Commun.*, **8**, 406 (2005).
[55] I.D. Brown, D. Altermatt. *Acta Crystallogr., Sect. B*, **B41**, 244 (1985).
[56] C.M. Liu, D.Q. Zhang, D.B. Zhu. *Cryst. Growth Des.*, **5**, 1639 (2005).
[57] A.K. Lyer, S.C. Peter. *Inorg. Chem.*, **53**, 653 (2014).
[58] J.G. Choi, L.T. Thompson. *Appl. Surf. Sci.*, **93**, 143 (1996).
[59] G.S. Yang, H.Y. Zang, Y.Q. Lan, X.L. Wang, C.J. Jiang, Z.M. Su, L.D. Zhu. *CrystEngComm.*, **13**, 1461 (2011).
[60] X.L. Wang, Y.F. Bi, B.K. Chen, H.Y. Lin, G.C. Liu. *Inorg. Chem.*, **47**, 2442 (2008).
[61] X.L. Wang, Q. Qao, A.X. Tian, D. Zhao, X.J. Liu. *J. Coord. Chem.*, **66**, 358 (2013).
[62] X.L. Wang, C. Qin, E.B. Wang, Z.M. Su, Y.G. Li, L. Xu. *Angew. Chem., Int. Ed.*., **45**, 7411 (2006).
[63] K. Somayeh, S. Esmaeil, B. Madalina. *J. Electroanal. Chem.*, **80**, 704 (2013).
[64] Y. Yu, H.J. Pang, H.Y. Ma, Y.B. Song, K. Wang. *J. Cluster Sci.*, **24**, 17 (2013).
[65] S.B. Li, W. Zhu, H.Y. Ma, H.J. Pang, H. Liu, T.T. Yu. *RSC Adv.*, **3**, 9730 (2013).
[66] B. Keita, A. Belhouari, L. Nadjo, R. Contant. *J. Electroanal. Chem.*, **381**, 243 (1995).